

# A process-based soil erosion model ensemble to assess model uncertainty in climate-change impact assessments

Joris P.C. Eekhout<sup>1</sup>  | Agustín Millares-Valenzuela<sup>2</sup> | Alberto Martínez-Salvador<sup>3</sup> | Rafael García-Lorenzo<sup>3</sup> | Pedro Pérez-Cutillas<sup>3</sup> | Carmelo Conesa-García<sup>3</sup> | Joris de Vente<sup>1</sup>

<sup>1</sup>Soil and Water Conservation Research Group, CEBAS-CSIC, Spanish Research Council, Murcia, Spain

<sup>2</sup>Group of Environmental Fluid Dynamics, Andalusian Institute for Earth System Research (IISTA), University of Granada, Granada, Spain

<sup>3</sup>Department of Geography, University of Murcia, Murcia, Spain

## Correspondence

Joris P.C. Eekhout, Soil and Water Conservation Research Group, CEBAS-CSIC, Spanish Research Council, Campus de Espinardo, 30100, PO Box 164, Murcia, Spain.  
 Email: joriseekhout@gmail.com

## Funding information

Ministerio de Ciencia e Innovación, Grant/Award Number: PID2019-109381RB-I00;  
 Ministerio de Ciencia, Innovación y Universidades, Grant/Award Number: CGL2017-84625-C2-1-R

## Abstract

The impact of climate change on future soil loss is commonly assessed with soil erosion models, which are suggested to be an important source of uncertainty. Here, we present a novel soil erosion model ensemble to assess model uncertainty in climate-change impact assessments. The model ensemble consists of five continuous process-based soil erosion models that run at a daily time step (i.e., DHSVM, HSPF, INCA, MMF, SHETRAN). The models were implemented in the SPHY hydrological model and simulate detachment by raindrop impact, detachment by runoff, and immediate deposition. The soil erosion model ensemble was applied in a semiarid catchment in the southeast of Spain. We applied three future climate scenarios based on global mean temperature rise (+1.5, +2 and +3°C). Data from two contrasting regional climate models were used to assess how an increase and a decrease in projected extreme precipitation affect model uncertainty. Soil loss is projected to increase (up to 95%) and decrease (up to -30%) under climate change, mostly reflecting the change in extreme precipitation. Model uncertainty is found to increase with increasing slope, extreme precipitation and runoff, which reveals some inherent differences in model assumptions among the five models. Moreover, the model uncertainty increases in all climate change scenarios, independent of the projected change in annual precipitation and extreme precipitation. This stresses the importance to consider model uncertainty through model ensembles of climate, hydrology, and soil erosion in climate-change impact assessments.

## KEY WORDS

climate change, model ensemble, model uncertainty, process-based, soil erosion

## 1 | INTRODUCTION

In many locations worldwide an increase of soil erosion is expected under climate change (Borrelli et al., 2020; Nearing, Pruski, & O'Neal, 2004), which is often associated with the projected increase in extreme precipitation (Sun, Solomon, Dai, & Portmann, 2007). The change in soil erosion under climate change is commonly assessed using a wide range of soil erosion models, from event-scale to annual

models and from process-based to empirical models (Eekhout & de Vente, 2020a; Li & Fang, 2016). Differences in model assumptions and conceptualizations may lead to opposing soil erosion projections by climate change (Eekhout & de Vente, 2020a); hence, it is crucial to select a soil erosion model that simulates the most relevant processes, considering how soil erosion processes are affected under future climate conditions. However, even the same type of soil erosion models can project differences in soil erosion rates of up to an order of

magnitude (Centeri, Barta, Jakab, Szalai, & Bíró, 2009). Therefore, in addition to often reported uncertainty due to differences in input data or model parametrization (Batista, Davies, Silva, & Quinton, 2019; Bussi et al., 2016; Cho, Wilcock, & Hobbs, 2018), it may be essential to use an ensemble of soil erosion models in climate-change impact assessments, to account for the uncertainties in projected soil loss that arise from the differences in soil erosion model assumptions.

Raindrop impact and runoff are the main detaching agents for soil erosion by water (Morgan, 2005). Detachment by raindrop impact is a function of the intensity, amount and size of the raindrops that reach the soil surface (Nearing, Deer-Ascough, & Lafren, 1990). Detachment by runoff occurs when the forces exerted by the flow of water exceed the forces keeping the soil particle at rest (Morgan, 2005). A hydrological model is required to simulate detachment by runoff, which significantly increases the model complexity, number of model parameters and input data requirements. Notwithstanding these limitations, many soil erosion models simulate both detachment by raindrop impact and runoff, and are applied in climate-change impact assessments, such as ANSWERS (Beasley, Huggins, & Monke, 1980), EUROSEM (Morgan et al., 1998a), INCA (Lazar et al., 2010), MEDRUSH (Kirkby, Abrahart, McMahon, Shao, & Thornes, 1998), MEFIDIS (Nunes, Vieira, Seixas, Gonçalves, & Carvalhais, 2005), RHEM (Nearing et al., 2011), SHETRAN (Ewen, Parkin, & O'Connell, 2000), SPHY-MMF (Eekhout, Terink, & de Vente, 2018) and WEPP (Nearing, Foster, Lane, & Finkner, 1989). While all these models simulate the two main detachment processes, there are still many differences, including the temporal scale (event-scale vs. continuous models), the time step (sub-hourly to daily) and the detail of the simulated processes (Pandey, Himanshu, Mishra, & Singh, 2016).

Simplifications, assumptions and choices of parametrizations have to be made when constructing a model, inevitably leading to errors in the model outcome (Tebaldi & Knutti, 2007). By combining several models in an ensemble, the errors originating from the model assumptions might at least partially cancel out, ultimately improving the confidence in the model outcome. By all means, this assumption depends on the size of the model ensemble and the range in model assumptions considered, where a larger model ensemble, consisting of a large variety of model assumptions, increases the confidence in the model outcome. Many sources of uncertainty are involved in climate change assessments on soil erosion, including the uncertainty arising from climate models, bias-correction methods and downscaling techniques (Eekhout & de Vente, 2019; Garbrecht, Nearing, Zhang, & Steiner, 2016; Mondal et al., 2015; Op de Hipt et al., 2018; Simonneaux et al., 2015). Soil erosion models are suggested to be a large source of uncertainty in climate-change impact assessments as well (Shrestha et al., 2013; Garbrecht et al., 2016; Li & Fang, 2016; Op de Hipt et al., 2018); however, only a few studies quantified this uncertainty. For instance, Bussi et al. (2016), Cho et al. (2018) and Batista et al. (2021) estimated model uncertainty related to model parametrization with a Monte Carlo-based approach, ultimately applying a selection of optimized parameter sets. Other sources of uncertainty are related to input data selection and model conceptualization (de Vente et al., 2013; Van Rompaey & Govers, 2002; van Rompaey,

Govers, & Baudet, 1999). While a model ensemble approach to assess model uncertainty is common in hydrological studies, including climate-change impact assessments on stream flow (Li et al., 2018; Zhao, Li, Cai, & Wang, 2020), floods (Thobor et al., 2018) and water resources (Teklesadik et al., 2017; Velázquez et al., 2013), such an approach has not been attempted in the context of soil erosion.

Previous studies showed that soil loss estimates from soil erosion models are inherently uncertain (Brazier, Beven, Freer, & Rowan, 2000; Quinton, 1997). While there are some exceptions related to uncertainty in input parameters and model comparisons (e.g., Batista et al., 2021; Falk, Denham, & Mengersen, 2010; Jetten, Govers, & Hessel, 2003; Schürz, Mehdi, Kiesel, Schulz, & Herrnegger, 2020), model uncertainty has received little attention as compared to uncertainty in hydrology and climate-change assessments (Beven & Brazier, 2011; Batista et al., 2019). Here, we propose a novel ensemble of continuous process-based soil erosion models, with the aim to assess the uncertainty from erosion model assumptions in climate-change impact assessments. We focus on process-based soil erosion models, because such models may be better suited to simulate the impact of climate change in the study area (Eekhout & de Vente, 2020a). Furthermore, we focus on continuous models with a daily time step, thereby maintaining the full detail provided by the climate model outcome and simplifying the preparation of climate forcing for the models. The proposed soil erosion model ensemble consists of five models: DHSVM (Doten, Bowling, Lanini, Maurer, & Lettenmaier, 2006), HSPF (Bicknell, Imhoff, Kittle, Donigian, & Johanson, 1993), INCA (Lazar et al., 2010), MMF (Eekhout, Terink, & de Vente, 2018) and SHETRAN (Lukey, Bathurst, Hiley, & Ewen, 1995). The soil erosion model ensemble was applied in the Upper Mula catchment, a semiarid catchment in the southeast of Spain. We applied three future climate scenarios based on global mean temperature rise (+1.5, +2 and +3°C). Data from two contrasting regional climate models were used to assess how increases and decreases in extreme precipitation affect model uncertainty.

## 2 | MATERIALS AND METHODS

### 2.1 | Soil erosion model ensemble

We applied an ensemble of five continuous process-based soil erosion models that run at a daily time step, that is, DHSVM, HSPF, INCA, MMF and SHETRAN. The models were implemented in the SPHY hydrological model (Terink, Lutz, Simons, Immerzeel, & Droogers, 2015), see below for more details on the hydrological model. All models simulate detachment by raindrop impact, detachment by runoff and immediate deposition of sediment within the cell of its origin (Table 1). Most models also simulate sediment transport and channel erosion/deposition, however, here we restrict our implementation and analysis to hillslope erosion processes. To prevent unrealistically high soil erosion rates by runoff processes, we also restricted the detachment by runoff processes to the catchment surface with a contributing area smaller than 0.1 km<sup>2</sup>, based on the

**TABLE 1** Soil erosion model characteristics and simulated processes

Simulated processes	DHSVM	HSPF	INCA	MMF	SHETRAN
Detachment by raindrop impact	×	×	×	×	×
Leaf drain	×			×	×
Direct throughfall	×			×	×
Detachment by runoff	×	×	×	×	×
Based on rill dimensions	×				×
Immediate deposition	×	×	×	×	×
Sediment storage		×	×		

characteristics of the drainage network of the study area. Detachment by raindrop impact is determined in the entire model domain. Below we provide a brief description of each of the five models. A full description can be found in Appendix S1 (Text S1) and the code is available on GitHub ([https://github.com/FutureWater/SPHY/tree/soil\\_erosion\\_ensemble](https://github.com/FutureWater/SPHY/tree/soil_erosion_ensemble); Eekhout & de Vente, 2020b).

### 2.1.1 | DHSVM

The distributed hydrology-soil-vegetation model (DHSVM) (Doten et al., 2006) simulates hillslope erosion based on detachment energy of raindrops, leaf drip and surface runoff. The detachment by raindrop impact formulations originate from the SHESED model (Wicks & Bathurst, 1996). These formulations require hourly precipitation intensity as input. While the SPHY hydrological model runs at a daily time step, the model includes a sub-daily infiltration formulation. This formulation determines hourly precipitation intensity, which was subsequently used as input for the DHSVM model. Furthermore, the detachment by raindrop impact formulations require the canopy cover as input, which was obtained from the vegetation module of the SPHY hydrological model.

Detachment by runoff is determined from a detachment coefficient, the settling velocity and the transport capacity. The detachment coefficient is a function of the soil cohesion, which is determined from the sum of the soil cohesion and root cohesion, with values obtained from Morgan et al. (1998b). The transport capacity is based on the unit stream power approach from the KINEROS model (Woolhiser, Smith, & Goodrich, 1990), which requires the water depth of the flow as input. We obtained the water depth by applying the Manning equation, assuming a triangular-shaped flow profile, with the width-depth ratio as model parameter.

### 2.1.2 | HSPF

The Hydrological Simulation Program-Fortran (HSPF) model (Bicknell et al., 1993) simulates detachment by raindrop impact with daily precipitation intensity as input. The soil erodibility is based on the USLE K-factor, here estimated using the method proposed by Wischmeier, Johnson, & Cross (1971). Detached sediment by raindrop impact is stored in the sediment storage, which decreases as a result of soil

crusting, simulated by a reduction parameter. The amount of detached sediment by raindrop impact taken into transport is a function of the sediment storage and the transport capacity. Detachment by runoff is a function of surface runoff and a coefficient for scour of the soil matrix.

### 2.1.3 | INCA

The Integrated Catchments model for Sediments (INCA-Sed) (Lazar et al., 2010) is originally applied in a semi-distributed manner, however, here the model is implemented in the spatially distributed SPHY hydrological model. Detachment by raindrop impact is a function of the daily precipitation intensity and the canopy cover, for which the latter is obtained from the vegetation module from the SPHY hydrological model. For model calibration purposes, we included the groundcover as a model parameter in the detachment by raindrop impact formulation. Detachment by runoff is a function of the sediment transport, the surface runoff and the detachment by raindrop impact. Sediment that is taken into transport is determined from the before mentioned formulations, accounting for sediment storage.

### 2.1.4 | MMF

The Morgan-Morgan-Finney model (MMF) (Morgan & Duzant, 2008) was originally implemented as an annual model, however, here, we applied the daily implementation by Eekhout, Terink, & de Vente (2018). The detachment by raindrop impact is a function of the highest daily precipitation intensity and the canopy cover, which are both obtained from the SPHY hydrological model. Detachment by runoff is a function of the accumulated runoff. Both detachment by raindrop impact and runoff are determined for each of the three textural classes (sand, silt and clay) separately and later aggregated to determine the total detachment. Immediate deposition is a function of the particle fall number, in which the flow velocity is determined with the Manning equation.

### 2.1.5 | SHETRAN

The SHETRAN model (Lukey et al., 1995) is a sediment transport model implemented in the Système Hydrologique Européen (SHE)

hydrological model. The detachment by raindrop impact formulations are similar to the ones used in DHSVM, with some small differences in the leaf drip formulations. The canopy cover is obtained from the vegetation module of the SPHY hydrological model. Detachment by runoff is a function of the shear stress and critical shear stress, which are both a function of the water depth. Similar to DHSVM, we obtained the water depth using the Manning equation, assuming a triangular-shaped flow profile, with the width-depth ratio as model parameter. For model calibration purposes, we included the groundcover as a model parameter in the detachment by runoff formulation. Immediate deposition of sediment is determined with a sediment transport equation, for which we adopted the equation by Engelund & Hansen (1967).

## 2.2 | Hydrological model

While each of the five models are originally implemented within their specific hydrological models, here we implemented all soil erosion models in the SPHY hydrological model (v3.0; Terink et al., 2015; Eekhout, Terink, & de Vente, 2018), a process-based and spatially distributed model. The model is applied with a daily time step. The hydrological model simulates most relevant hydrological processes, such as evapotranspiration, infiltration and saturation excess surface runoff, and lateral and vertical soil moisture flow. The model also incorporates a vegetation module, which determines actual evapotranspiration, interception, canopy storage, throughfall and canopy cover, and is based on the spatial and temporal variation of Normalized Differenced Vegetation Index (NDVI).

## 2.3 | Study area

The study was performed in the Upper Mula catchment ( $169.6 \text{ km}^2$ ), a subcatchment of the Segura River basin, located in the southeast of Spain (Figure 1 and Table 2). The study area is predominantly classified as semiarid, with an average annual precipitation sum of 399 mm (1971–2000; Serrano-Notivoli, Beguería, Saz, Longares, & de Luis, 2017) and an average temperature of  $15.7^\circ\text{C}$  (1971–2000; Herrera, Fernández, & Gutiérrez, 2016). The catchment can be considered a mixed catchment, where forest (33.0%), rainfed tree crops (25.3%) and shrubland (24.5%) are the most dominant land use classes.

## 2.4 | Calibration

### 2.4.1 | Hydrological model

The hydrological model was calibrated at the catchment outlet, using daily observed discharge data obtained for the period 2002–2007 and evaluated for the period 1997–2001. We adopted a two-step procedure to calibrate the hydrological model. First, we optimized the percent bias (PBIAS) for annual discharge, optimizing model parameters related to the soil hydraulic properties and the thickness of the soil. Second, we optimized the Kling-Gupta model efficiency (KGE) (Gupta, Kling, Yilmaz, & Martinez, 2009) for daily discharge, which has an optimum at 1. In the second step, we optimized a model parameter from the routing module. See Table S6 for the optimized values of the model parameters used in the calibration of the hydrological model.

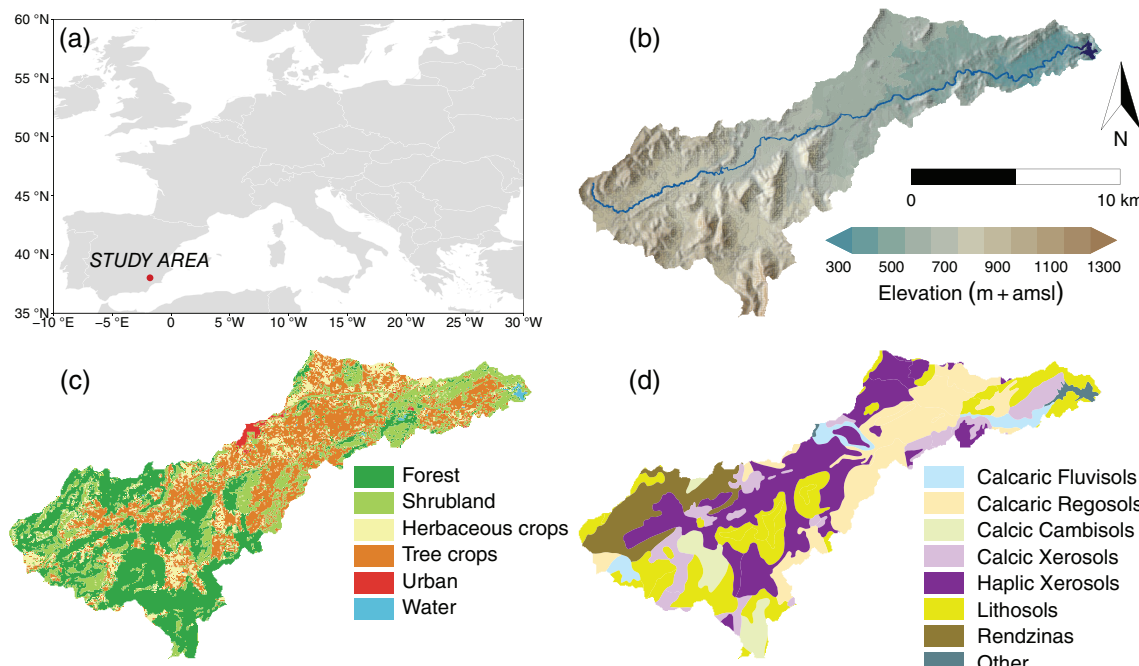


**FIGURE 1** Location and characteristics of the upper Mula catchment: (a) location of the study area within Europe, (b) Digital Elevation Model (Ministerio de Fomento de España, 2015), (c) land use map (Rodríguez-Valero & Alonso-Sarria, 2019), and (d) soil class map (Faz Cano, 2003) [Colour figure can be viewed at [wileyonlinelibrary.com](http://wileyonlinelibrary.com)]

**TABLE 2** Characteristics of the upper Mula catchment

	Characteristics
Area (km <sup>2</sup> )	169.6
Mean annual precipitation sum (mm)	399.1
Average temperature (°C)	15.7
Dominant Köppen class (area)	BSk (86.2%)
Minimum elevation (m)	347.2
Maximum elevation (m)	1,374.3
Average slope (m m <sup>-1</sup> )	0.17
Land use distribution:	
Forest (%)	33.0
Shrubland (%)	24.5
Rainfed tree crops (%)	25.3
Irrigated tree crops (%)	4.0
Cereals (%)	10.7
Horticulture (%)	1.4
Urban (%)	0.7
Water (%)	0.3

**TABLE 3** Climate models (GCM/RCM combinations) and their corresponding periods per temperature scenario

GCM/RCM	+1.5°C	+2.0°C	+3.0°C
MPI-ESM-LR/RCA	2013–2042	2029–2058	2052–2081
EC-EARTH/CCLM	2012–2041	2028–2057	2052–2081

The calibration resulted in a PBIAS of 0.0 and a KGE of 0.58 and the evaluation in a PBIAS of –27.6 and a KGE of 0.13 (Figure S1).

#### 2.4.2 | Soil erosion models

The soil erosion models were calibrated for the period 2002–2007 and evaluated for the period 1997–2001. The calibration focussed on two indicators, that is, the ratio between detachment by raindrop

impact and detachment by runoff, and the soil erosion rates of the four main land use classes, that is, forest, herbaceous crops, tree crops and shrubland. While the ratio between detachment by raindrop impact and detachment by runoff depends on many factors, previous research showed that detachment by runoff prevails over detachment by raindrop impact (Cerdan, Le Bissonnais, Couturier, Bourennane, & Souchère, 2002; Morgan, 2005; Kimaro, Poesen, Msanya, & Deckers, 2008; Liu, Zhang, & Yang, 2011; Sun, Fang, Qi, Li, & Cai, 2013; Xiao et al., 2017). We adopted a ratio of 30:70 (raindrop impact:runoff), which is a consensus of the before mentioned publications. The calibration of the soil erosion rates per land use class was based on a large review of plot-scale soil loss data for the Mediterranean region obtained from Maetens et al. (2012).

We adopted a two-step calibration procedure to calibrate the soil erosion models. First, we calibrated the model parameters related to soil erodibility and transport capacity in the area covered by tree crops. We focussed on tree crops because we assume that their groundcover is negligible due to frequent ploughing, hence, land use specific model parameters (as used in the second step) cannot be used to calibrate the soil loss for tree crops. In this first step, we calibrated the ratio between detachment by raindrop impact and detachment by runoff, simultaneously accounting for the soil erosion rates for tree crops obtained from Maetens et al. (2012). See Table S7 for the optimized values for each of the five soil erosion models. In the second step, we calibrated the soil erosion rates for the three other main land use classes, that is, forest, herbaceous crops and shrubland, using land use specific model parameters, such as groundcover. See Table S8 for the optimized values per soil erosion model for each of the four land use classes. The soil erosion rates from Maetens et al. (2012) were obtained in erosion plots with a maximum length of 200 m, hence, we only included those grid cells that have an accumulated slope length of up to 200 m. For the calibration of the soil erosion rates per land use class, we determined the annual unit soil loss, which is soil loss corrected for slope gradient and plot length (Bagarello, Ferro, & Giordano, 2010). The land use specific model parameters were adjusted such that the average annual soil loss was within 1% of the literature values (see last row of Table 4).

**TABLE 4** Evaluation of annual unit soil loss (Mg km<sup>-2</sup> yr<sup>-1</sup>) and comparison with literature data from Maetens et al. (2012), with the percent bias shown between parentheses

Model	Forest <sup>a</sup>	Herbaceous crops	Tree crops	Shrubland	Ratio raindrop:Runoff
DHSVM	26.7 (–33.2%)	246.9 (7.4%)	322.0 (7.3%)	31.3 (4.3%)	20:80
HSPF	32.0 (–20.0%)	200.4 (–12.9%)	288.3 (–3.9%)	28.3 (–5.7%)	28:72
INCA	21.3 (–46.8%)	153.5 (–33.2%)	204.3 (–31.9%)	19.3 (–35.8%)	41:59
MMF	35.4 (–11.4%)	363.6 (58.1%)	446.3 (48.8%)	39.1 (30.2%)	21:79
SHETRAN	26.3 (–34.4%)	137.7 (–40.1%)	193.8 (–35.4%)	18.5 (–38.4%)	41:59
<b>Ensemble median</b>	<b>19.9 (–50.3%)</b>	<b>161.1 (–29.9%)</b>	<b>244.8 (–18.4%)</b>	<b>22.3 (–25.6%)</b>	
Literature	40.0	230.0	300.0	30.0	30:70

<sup>a</sup>Annual unit soil loss not available in Maetens et al. (2012), we used annual soil loss instead

Note: The last column shows the ratio between detachment by raindrop impact and detachment by runoff for the area with an accumulated slope length of up to 200 m

**TABLE 5** Annual precipitation sum (mm) and extreme precipitation (mm) for the reference scenario and changes between the reference scenario and the future scenarios, with percentage change between parentheses

	Reference	+1.5°C	+2.0°C	+3.0°C
<b>MPI-ESM-LR/RCA</b>				
Precipitation sum (mm)	399.1	-23.2 (-5.8%)	-91.4 (-22.9%)	-138.1 (-34.6%)
Extreme precipitation (mm)	36.9	0.8 (2.1%)	-5.7 (-15.5%)	-7.4 (-20.0%)
<b>EC-EARTH/CCLM</b>				
Precipitation sum (mm)	399.1	28.2 (7.1%)	10.5 (2.6%)	-62.2 (-15.6%)
Extreme precipitation (mm)	36.9	6.3 (17.1%)	9.6 (26.1%)	6.1 (16.6%)

Note: Extreme precipitation is defined as the 95th percentile of daily precipitation, considering only rainy days ( $>1 \text{ mm day}^{-1}$ ; Jacob et al., 2014)

## 2.5 | Input data

We applied the soil erosion model ensemble to a reference scenario (1971–2000) and three future climate scenarios, based on 1.5, 2 and 3°C global mean temperature rise. Climate data were obtained from two GCM/RCM (General Circulation Model/Regional Climate Model) combinations from the EURO-CORDEX initiative (Jacob et al., 2014), with a 0.11° resolution. We used climate projections for the RCP8.5 Representative Concentration Pathway. We selected the two climate models (MPI-ESM-LR/RCA and EC-EARTH/CCLM) based on their contrasting future projections in extreme precipitation (Table 5). We applied the method by Vautard et al. (2014) to determine the year when the two GCMs reach the defined increase in global mean temperature relative to preindustrial levels (1881–1910). Then, we defined the 30-year periods centred around these years as input for the soil erosion model ensemble (Table 3).

All input maps were interpolated or resampled to the 50 m model resolution. Precipitation and temperature data for the reference period (1971–2000) were obtained from the SPREAD daily dataset (Serrano-Notivoli et al., 2017, 5 km resolution) and the SPAIN02 daily dataset (Herrera et al., 2016, 0.11° resolution), respectively. The climate data were interpolated on the model grid using bilinear interpolation. The future climate model data were bias-corrected using scaled distribution mapping (Switanek et al., 2017), which scales the observed precipitation distribution by raw model projected changes in magnitude, rain-day frequency, and likelihood of events. This method was selected because it best reproduces the raw climate-change signal in the study area (Eekhout & de Vente, 2019). All other input data are described in Appendix S1 (Text S2).

## 2.6 | Uncertainty analysis

We determined the significance of the soil erosion model ensemble projections using a paired *U*-test (Mann–Whitney–Wilcoxon test). The paired *U*-test was applied on a cell-by-cell basis, from which the pairs consisted of the model output from each individual soil erosion model for the reference and the future scenario. Since the data are not normally distributed, we quantified the uncertainty from model assumptions of

the simulated soil loss using the coefficient of dispersion *CD*, which is defined as follows:

$$CD = \frac{Q_3 - Q_1}{Md}, \quad (1)$$

Where:  $Q_3$  is the third quartile,  $Q_1$  is the first quartile and  $Md$  is the median. We use the term model uncertainty to refer to the uncertainty from model assumptions only and not to other sources of model uncertainty, such as uncertainty from model parameterization or from input data.

## 3 | RESULTS

### 3.1 | Soil erosion model evaluation

All models underestimated soil loss for forest in the evaluation period, most notably the INCA model which shows the largest deviation from the literature value (Table 4). For the other land use classes, some models overestimate soil loss (DHSVM, MMF) while others underestimate soil loss (HSPF, INCA, SHETRAN). MMF and SHETRAN, respectively, over- and underestimates soil loss most. DHSVM and HSPF show least deviation from the literature values, within 15% for most land use classes. The ensemble median underestimates the soil loss for all land use classes. Forest is underestimated most (-50.3%), for which each of the five models underestimate soil loss. For the other land use classes, the deviation from the literature values is around 20–30%. HSPF shows the least deviation from the calibrated ratio between detachment by raindrop impact and runoff. Generally speaking, all models perform reasonably well with respect to this ratio, which ranges between 20:80 for DHSVM and 41:59 for INCA and SHETRAN.

### 3.2 | Climate

In the reference scenario, annual precipitation sum amounts to 399.1 mm and extreme precipitation, defined as the 95th percentile of daily precipitation, considering only rainy days ( $>1 \text{ mm day}^{-1}$ ; Jacob et al., 2014), amounts to 36.9 mm. There is a distinct gradient

between the catchment outlet and headwaters, where annual precipitation sum ranges between 320 and 530 mm and extreme precipitation between 31 and 51 mm (Figures S2 and S3).

We selected two GCM/RCM combinations that differ in projected change in annual precipitation sum and extreme precipitation. The MPI-ESM-LR/RCA climate model projects a decrease in precipitation sum for all three temperature scenarios, mainly in the headwaters of the catchment (Table 5 and Figure S2). Extreme precipitation is projected to slightly increase in the +1.5°C scenario, but decreases in the other two scenarios, with a maximum catchment-average of 20.0% in the +3.0°C scenario, also mainly in the headwaters of the catchment (Figure S3). The EC-EARTH/CCLM climate model projects an increase in precipitation sum in the +1.5 and +2.0°C scenarios, mainly in the downstream part of the catchment, and a decrease in the +3.0°C scenario. Extreme precipitation is projected to increase in all scenarios, with a maximum of 26.1% in the +2.0°C scenario.

### 3.3 | Soil loss projections

The ensemble median soil loss in the reference scenario is characterized by a patchy pattern of low and high soil loss rates (Figure 2), which mainly corresponds to the patchy land use pattern

(Figure 1c). The highest soil loss rates are recorded in agricultural areas and in those areas where most water accumulates. The five soil erosion models show considerable differences in the spatial variability of annual soil loss, which is manifested by the spread of the soil loss predictions (Figure 3). MMF shows the highest spatial variability among the five soil erosion models and INCA the lowest. The catchment median soil loss varies between 193.1 Mg km<sup>-2</sup> yr<sup>-1</sup> (DHSVM) and 316.8 Mg km<sup>-2</sup> yr<sup>-1</sup> (HSPF), while the catchment median soil loss for the ensemble median amounts to 231.7 Mg km<sup>-2</sup> yr<sup>-1</sup>.

Soil loss is projected to increase and decrease under climate change, depending on the temperature change scenario and on the climate model used. Most increase in soil loss is projected in the +1.5°C scenario for the EC-EARTH/CCLM climate model, with an ensemble median increase of 94.5% (Figure 4). In general, the change in ensemble median soil loss corresponds to the change in extreme precipitation, where soil loss is projected to increase in the scenarios where extreme precipitation is projected to increase and vice versa.

The direction of change is consistent among the five soil erosion models, except for the +2.0 and +3.0°C scenarios of the MPI-ESM-LR/RCA climate model, where DHSVM and MMF project a slight increase of soil loss, in contrast to a slight decrease as

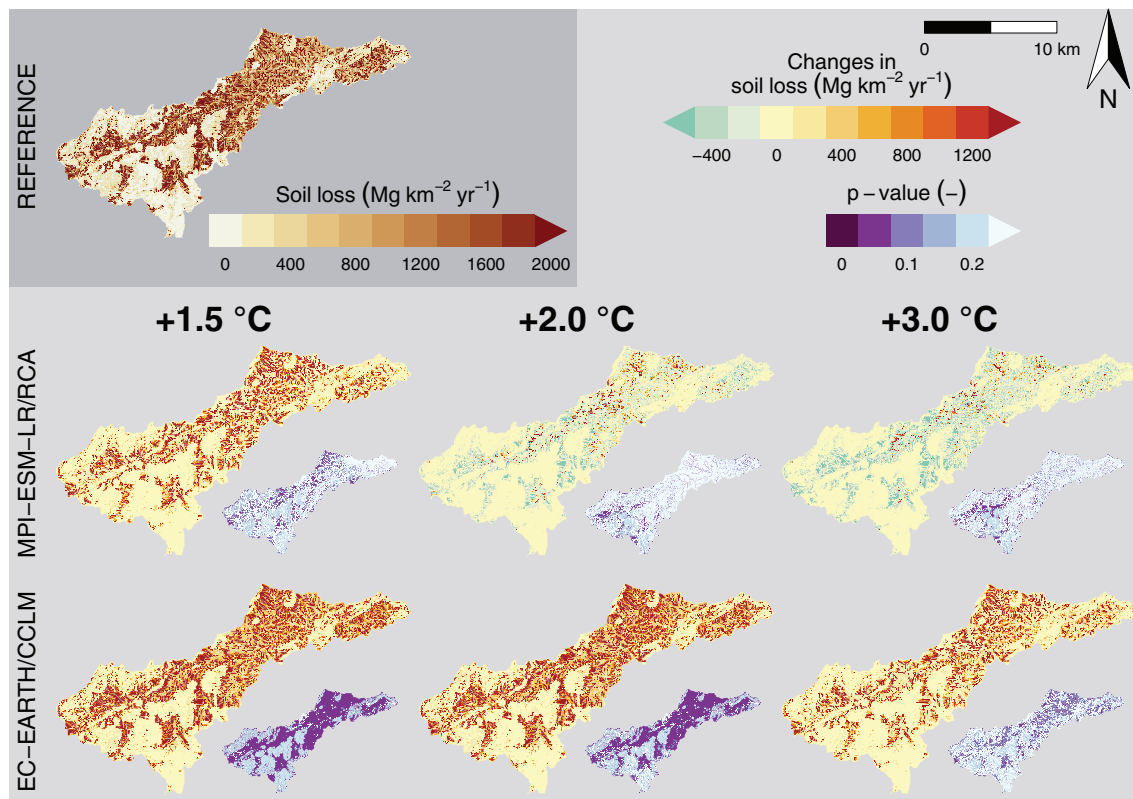


**FIGURE 2** Ensemble median annual soil loss (Mg km<sup>-2</sup> yr<sup>-1</sup>) for the reference scenario (1971–2000; top) and changes between the reference scenario and the future scenarios (MPI-ESM-LR/RCA, middle; EC-EARTH/CCLM, below). The small maps in the right bottom corner of each map shows the *p*-values obtained from the soil erosion model ensemble, where darker purple colours indicate more significant results [Colour figure can be viewed at [wileyonlinelibrary.com](http://wileyonlinelibrary.com)]

projected by the other models. DHSVM projects the highest increase of soil loss among the five soil erosion models, up to 310.2% in the +1.5°C scenarios for the EC-EARTH/CCLM climate model. INCA projects the lowest increase of soil loss in the scenarios where extreme precipitation is projected to increase. SHETRAN projects the most decrease in soil loss in the scenarios where extreme precipitation is projected to decrease. All models project an increase of soil loss in the two scenarios where annual precipitation is projected to decrease, but extreme precipitation to increase, that is, the +1.5°C scenario for the MPI-ESM-LR/RCA climate model and the +3.0°C scenario for the EC-EARTH/CCLM climate model.

### 3.4 | Uncertainty analysis

In the reference scenario, there is a distinction between the headwaters, where the coefficient of dispersion within the soil erosion model ensemble is high, and the downstream area, with a lower coefficient of dispersion (Figure 6). Among the four main land use classes, forest and

shrubland show more variation within the soil erosion model ensemble than herbaceous crops and tree crops, considering the median coefficient of dispersion (Figure 5). The other main model inputs show a gradient in the coefficient of dispersion, which increases with increasing slope, extreme precipitation and runoff, however, the gradients are most pronounced for runoff. The higher coefficient of dispersion for the natural land use classes may also be explained by the fact that forest and, to a lesser degree, shrubland are often found at steeper slopes.

The coefficient of dispersion increases in the future climate scenarios with respect to the reference scenario (Figure 6), meaning that soil erosion predictions under climate change become more uncertain. The coefficient of dispersion increases especially in the downstream area for the MPI-ESM-LR/RCA climate model and shows small or no change in the headwaters. For the EC-EARTH/CCLM climate model, the change in the coefficient of dispersion is more heterogeneously distributed over the catchment. The difference in the observed patterns of the coefficient of dispersion between the two climate models is most likely related to the difference in the spatial patterns of the projected change in annual precipitation sum and extreme precipitation (Figures S2 and S3). The catchment-average coefficient of dispersion increases most in the +1.5°C scenario for the MPI-ESM-LR/RCA climate model, amounting to  $CD = 1.28$ .

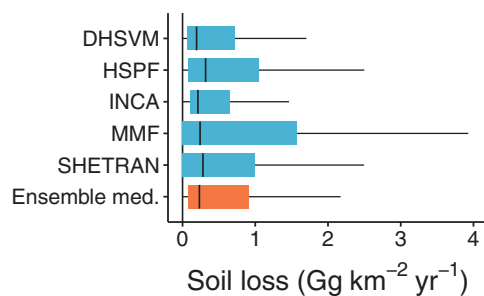


**FIGURE 3** Catchment-wide variability of the annual soil loss ( $\text{Gg km}^{-2} \text{yr}^{-1}$ ) for the reference scenario (1971–2000). The coloured boxes indicate the inter-quartile range (IQR) and the whiskers extend to  $\pm 1.5$  IQR [Colour figure can be viewed at [wileyonlinelibrary.com](http://wileyonlinelibrary.com)]

## 4 | DISCUSSION

### 4.1 | Ensemble predictions under climate change

Here, we present the application of a soil erosion model ensemble to account for the uncertainty from model assumptions, which is suggested to be an important source of uncertainty in climate-change impact assessments on soil erosion (Shrestha et al., 2013; Garbrecht et al., 2016; Li & Fang, 2016; Op de Hipt et al., 2018). The model ensemble consists of five continuous process-based soil erosion models, which all account for the main detachment agents (i.e., raindrop impact and runoff) and immediate deposition on

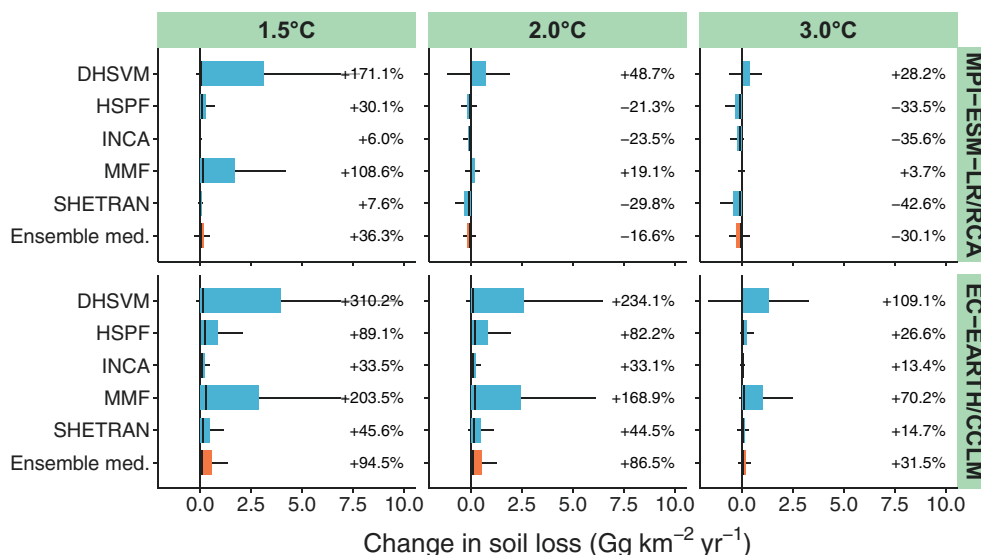


**FIGURE 4** Change in annual soil loss ( $\text{Gg km}^{-2} \text{yr}^{-1}$ ) between the reference scenario and the future scenarios (MPI-ESM-LR/RCA, middle; EC-EARTH/CCLM, below). The average change is shown in percentages. The colored boxes indicate the inter-quartile range (IQR) and the whiskers extend to  $\pm 1.5$  IQR [Colour figure can be viewed at [wileyonlinelibrary.com](http://wileyonlinelibrary.com)]

**FIGURE 5** Uncertainty from model assumptions, quantified with the coefficient of dispersion ( $-$ ) from the soil erosion model ensemble, for the reference scenario (1971–2000). The model uncertainty was determined for the four main land use classes, for five slope classes, for five extreme precipitation classes and for five runoff classes. The coloured boxes indicate the interquantile range (IQR) and the whiskers extend to  $\pm 1.5$  IQR [Colour figure can be viewed at [wileyonlinelibrary.com](http://wileyonlinelibrary.com)]

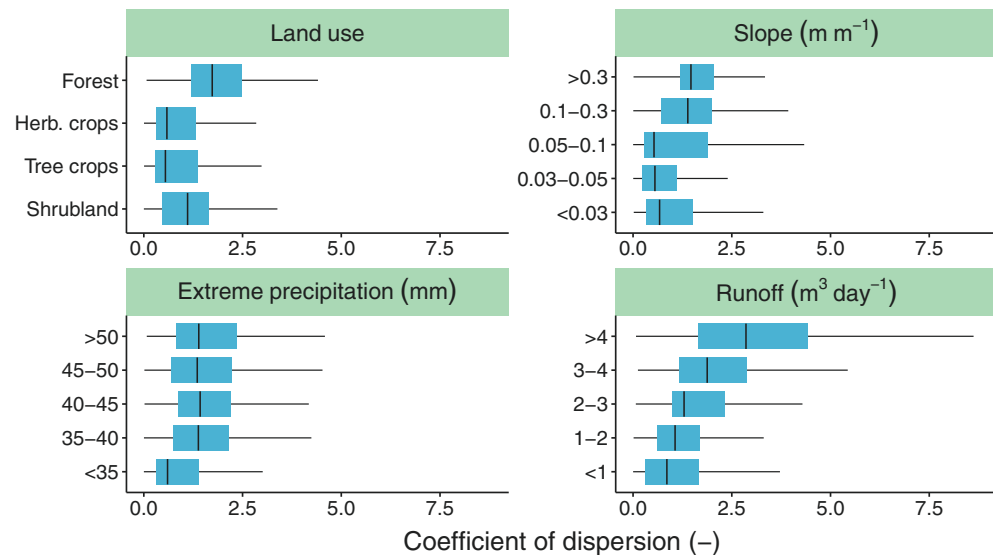
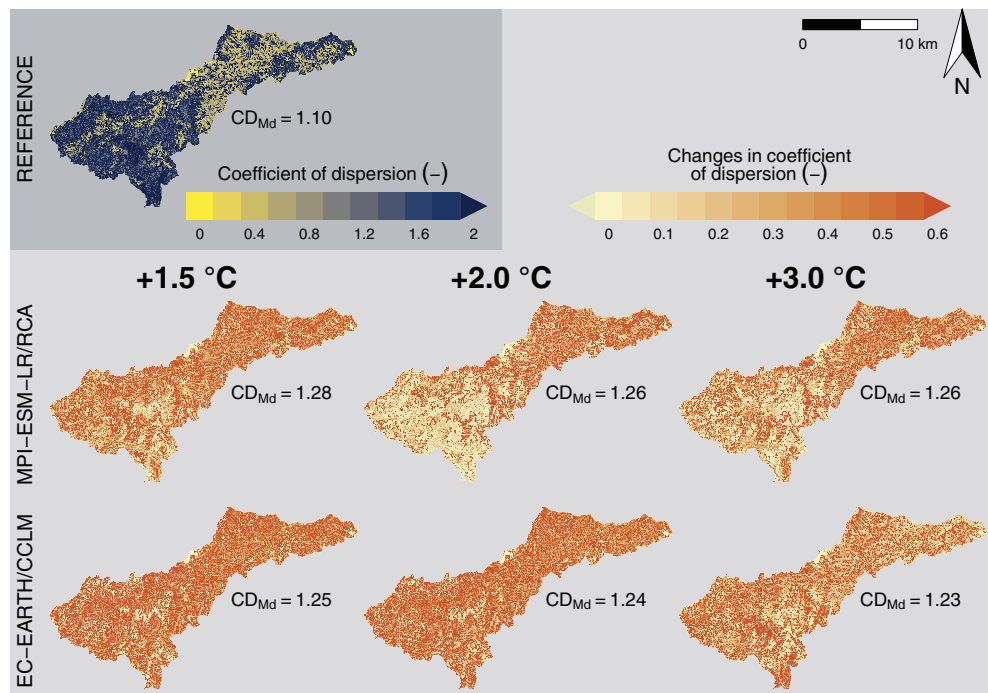


**FIGURE 6** Uncertainty from model assumptions, quantified with the coefficient of dispersion ( $-$ ) obtained from the soil erosion model ensemble, for the reference scenario (1971–2000; top) and changes between the reference scenario and the future scenarios (MPI-ESM-LR/RCA, middle; EC-EARTH/CCLM, below) [Colour figure can be viewed at [wileyonlinelibrary.com](http://wileyonlinelibrary.com)]



hillslopes (Table 1). Our results show that indeed there is a lot of variation within the model ensemble (Figure 6), which confirms the importance to account for model uncertainty under current and future climate conditions. In the reference scenario, the uncertainty increases with increasing slope, extreme precipitation and runoff (Figure 5), as a consequence of the differences in model assumptions. For instance, in some models, slope is explicitly used in the model formulations considering slope gradient (DHSVM, MMF, SHETTRAN), only considered through the slope length (INCA), or not considered at all (HSPF). Extreme precipitation is either approximated by hourly (DSHVM, MMF, SHETTRAN) or daily rainfall intensity (HSPF, INCA). The impact of (accumulated) runoff on soil detachment depends on the exponent considered in the detachment by runoff formulations,

which can either be smaller than 1 (INCA), equal to 1 (DHSVM, HSPF) or larger than 1 (MMF). This exponent will largely determine the prevalence of detachment by runoff in total soil erosion as compared to detachment by raindrop impact, especially in those areas where most water accumulates. Hence, we argue that using a model ensemble may be an effective method to account for model uncertainty because of the inherent differences in model assumptions.

To test how model uncertainty behaves under different climate-change projections, we selected two GCM/RCM combinations from the available models of the EURO-CORDEX initiative, for which extreme precipitation is projected to either increase or decrease most in the study area. By selecting these two contrasting climate models, we aimed to assess the sensitivity of erosion predictions and their

uncertainty to climate change. Under the reference scenario, we found that uncertainty increases with precipitation intensity (Figure 5), therefore, we hypothesized that the model uncertainty would not increase or even decrease in the scenarios where extreme precipitation is projected to decrease. However, the model uncertainty increases in all scenarios, independent of the projected change in annual and extreme precipitation (Figure 6). The model uncertainty increases less or seems stable in the headwaters of the +2.0 and +3.0°C scenarios of the MPI-ESM-LR/RCA climate model, where extreme precipitation is projected to decrease most. However, the model uncertainty in this area was already high in the reference scenarios, so it did not have much impact on the catchment average model uncertainty. Climate change will most likely cause an increase in extreme precipitation in many locations worldwide (Sun et al., 2007), which is often associated with a future increase in soil erosion (Nearing et al., 2004; Nunes, Seixas, & Pacheco, 2008; Mullan, Favis-Mortlock, & Fealy, 2012; Baartman, Jetten, Ritsema, & de Vente, 2012). An increase in extreme precipitation is also often associated with an increase in surface runoff, especially where infiltration excess is the dominant surface runoff mechanism (Eekhout, Hunink, Terink, & de Vente, 2018). As discussed before, extreme precipitation and runoff are found to be correlated with model uncertainty (Figure 5), which supports the claim that soil erosion uncertainty from model assumptions should be accounted for in climate-change impact assessments.

## 4.2 | Calibration procedure

The calibration procedure employed in this case-study, which partly consisted in calibrating the ratio between detachment by raindrop impact and detachment by runoff, may also have affected the model uncertainty. The ratio was mainly calibrated by adjusting the soil erodibility parameters, which are parameterized for raindrop impact and runoff, separately. The erodibility parameters may be obtained from field measurements for DHSVM, MMF and SHETRAN; however, most model descriptions and model applications suggest to use these parameters for calibration purposes. We calibrated the models with the ratio between detachment by raindrop impact and runoff, with the aim to apply a uniform calibration strategy for all five models.

The ratio we employed (30:70) was a consensus of the few studies available on this subject (i.e., Cerdan et al., 2002; Morgan, 2005; Kimaro et al., 2008; Liu et al., 2011; Sun et al., 2013; Xiao et al., 2017). Of course, this is open for debate, especially because most of these studies were performed at the plot- or laboratory-scale and not at the catchment-scale where the current study applies. We calibrated the models in the part of the catchment with a maximum slope length of 200 m, corresponding to the maximum plot length from Maetens et al. (2012). Due to the accumulation of water, runoff increases in downstream direction, so at the catchment-scale the ratio would obviously shift towards detachment by runoff. This behaviour is apparent for all models (Figures S4 and S5). The catchment-scale ratio for HSPF, INCA and SHETRAN slightly shifted towards

detachment by runoff, however, DHSVM and MMF are completely dominated by detachment by runoff at the catchment-scale. Ultimately, the catchment-scale soil loss is projected to increase in all scenarios for DHSVM and MMF, even in those scenarios where annual precipitation sum and extreme precipitation are projected to decrease (Figure 4). This might suggest that DHSVM and MMF are sensitive to extreme events that are not captured by the extreme precipitation indicator used here (i.e., the 95th percentile of daily precipitation), which generate a significant amount of runoff, increasing detachment by runoff under climate change.

## 4.3 | Uncertainty cascade

There are multiple sources of uncertainty involved in climate-change impact assessments. The soil erosion model uncertainty comes at the end of the modelling chain, which is also known as the 'uncertainty cascade' (Coulthard, Ramirez, Fowler, & Glenis, 2012). In the case of climate-change impact assessments, this cascade includes general circulation models, regional climate models, bias-correction methods, downscaling techniques, hydrological models and, ultimately, soil erosion models (Coulthard et al., 2012; Eekhout & de Vente, 2019; Garbrecht et al., 2016; Mondal et al., 2015; Op de Hipt et al., 2018; Scholz, Quinton, & Strauss, 2008; Simonneaux et al., 2015). Most recent climate-change impact assessments on soil erosion account for climate model uncertainty through the use of a climate model ensemble (GCM or RCM) (Eekhout & de Vente, 2019). The two GCM/RCM combinations used here project opposing impacts on annual precipitation and extreme precipitation for the same temperature scenarios (Table 5), confirming climate models as an important source of uncertainty in soil erosion impact assessments (Zabaleta, Meaurio, Ruiz, & Antigüedad, 2014; Azari, Moradi, Saghafian, & Faramarzi, 2016; D. P. Shrestha & Jetten, 2018; Amanambu et al., 2019). Bias-correction and downscaling are needed to make climate model output applicable in hydrological and soil erosion models, which are demonstrated to have a meaningful impact on soil loss projections (Eekhout & de Vente, 2019; Mondal et al., 2015; Simonneaux et al., 2015). However, each technique may be evaluated with historical climate observations or the raw climate signal from the climate models, through which the best technique can be selected. For instance, Eekhout and de Vente (2019) showed that scaled distribution mapping best reproduces the raw climate-change signal in the study area, therefore, we applied this bias-correction method here.

Model uncertainty of hydrological models may originate from several sources, including uncertainty in the model input, such as climate and land use, model assumptions and model parameterization (Samaniego et al., 2017). Many recent climate-change impact assessments use hydrological model ensembles to account for model uncertainty (e.g., Li et al., 2018; Teklesadik et al., 2017; Thober et al., 2018; Velázquez et al., 2013; Zhao et al., 2020). Samaniego et al. (2017) showed that climate model uncertainty dominates over hydrological model uncertainty, but suggested that hydrological model uncertainty should be accounted for in climate-change impact assessments. While

we only used two climate models in this study, our results highlight that climate models indeed include much uncertainty. For instance, an opposite change in ensemble-median soil loss is projected for the +3.0°C scenario, that is, -30.1% for MPI-ESM-LR/RCA and +31.5% for EC-EARTH/CCLM (Figure 4). Whether the uncertainty in the soil loss projections is dominated by climate model uncertainty or soil erosion model uncertainty cannot be concluded from this study, because of the limited number of climate models employed here. A similar analysis as performed by Samaniego et al. (2017), where multiple climate models and soil erosion models are considered, would be an interesting opportunity for future research. This could also be extended with a hydrological model ensemble, for instance through a similar approach as used in the ISIMIP project (Warszawski et al., 2014), where multiple climate and hydrological models have been applied to 12 large catchments worldwide. The ISIMIP project revealed that uncertainty from climate and hydrological models is also dependent on geographical region and climate (Krysanova et al., 2017). This must certainly be true for soil erosion models, where the occurrence and impact of erosive rain varies substantially across the globe, for example, due to interactions and feedbacks with vegetation cover (Morgan, 2005).

Soil erosion models can be found at the end of the uncertainty cascade. Uncertainty is not frequently considered in soil erosion model assessments (Alewell, Borrelli, Meusburger, & Panagos, 2019; Batista et al., 2019), beyond uncertainty in model input data or uncertainty in model parameterization (e.g., Batista et al., 2021; Schürz et al., 2020). Similar to hydrological models, uncertainty in soil erosion models may originate from input data, model assumptions and model parameterization. Here, we focussed on the uncertainty from model assumptions through the use of a soil erosion model ensemble. While our ensemble consisted of five continuous process-based models, a similar approach may be applicable for other model types, such as event-based or empirical models. However, we argue that such an ensemble should be restricted to a single type of soil erosion model, based on similar general model assumptions, such as employed here. An ensemble of, for example, process-based models that determine net erosion (difference between erosion and deposition) and empirical models that determine gross erosion (without deposition) would probably lead to meaningless results. This is highlighted by previous studies that conclude that contrasting model assumptions, representing different erosion and deposition processes, often lead to opposing soil loss estimates (Chandramohan, Venkatesh, & Balchand, 2015; Croke & Nethery, 2006; de Vente et al., 2013; Eekhout & de Vente, 2020a; Stolpe, 2005; Tiwari, Risse, & Nearing, 2000). Uncertainty in model parameterization may originate from measurement errors and the calibration procedure (Batista et al., 2019). In general, multiple parameter sets exist that could potentially lead to acceptable model performance (equifinality; Beven, 2006). These are difficulties that should be dealt with in any model assessment, also when applying a single model. The impact of input data selection on erosion assessments has been reported in several studies (e.g., de Vente, Poesen, Govers, & Boix-Fayos, 2009; Schürz et al., 2020), whereas the

uncertainty arising from model calibration has not received much attention in soil erosion model assessments (Batista et al., 2019). Probabilistic approaches may be employed to account for the uncertainty from model parameterization (Batista et al., 2019; Bussi et al., 2016; Cho et al., 2018). Because of the multiple sources of model uncertainty involved, the application of an ensemble of soil erosion models provides only a partial quantification of model uncertainty. To get a complete picture, future research could involve the application of a soil erosion model ensemble in combination with probabilistic approaches to account for uncertainty from model parameterization.

## 5 | CONCLUSIONS

Uncertainty from model assumptions has not received much attention in soil erosion model assessments. We quantified the uncertainty from model assumptions in a climate-change impact assessment through the use of a soil erosion model ensemble, which consists of five continuous process-based soil erosion models, that is, DHSVM, HSPF, INCA, MMF and SHETRAN. All models account for the detachment by raindrop impact, detachment by runoff and immediate deposition. Considering the process-based nature of the five models, we consider all soil erosion models capable of being applied in climate-change impact assessments. Model uncertainty was found to increase with increasing slope, extreme precipitation and runoff, which reveals some inherent differences in model assumptions among the five models. Hence, we argue that a model ensemble may be an effective method to assess model uncertainty because of their inherent differences in model assumptions. An increase in extreme precipitation is projected for the future, which may also be associated with an increase in runoff. Accordingly, the use of a model ensemble may be even more important in climate-change impact assessments. This is confirmed by the fact that the model uncertainty increases in all climate-change scenarios, with respect to the reference scenario. While the increase in model uncertainty may partly be related to the calibration procedure employed here, we argue that the way how extreme precipitation and runoff are used to force the soil erosion models plays a significant role, as well. This supports our claim to consider model uncertainty through model ensembles of climate, hydrology and soil erosion in climate-change impact assessments in addition to uncertainty from input data and model parameterization. Our findings and approach help to quantify the range of erosion risks that we are facing under climate change considering the available knowledge provided by continuous process-based soil erosion models.

## ACKNOWLEDGMENTS

This work has been financed by ERDF/Spanish Ministry of Science, Innovation and Universities—State Research Agency/Project CGL2017-84625-C2-1-R (CCAMICEM) and Project PID2019-109381RB-I00/AEI/10.13039/501100011033 (XTREME) both under the

National Program for Research, Development and Innovation focused on the Societal Challenges. The authors thank AEMET and UC for the data provided for this work Spain02 v5 dataset, available at <http://www.meteo.unican.es/datasets/spain02>.

## DATA AVAILABILITY STATEMENT

The model output data that support the findings of this study are available from the corresponding author upon reasonable request.

## ORCID

Joris P.C. Eekhout  <https://orcid.org/0000-0003-2097-696X>

## REFERENCES

- Aleweli, C., Borrelli, P., Meusburger, K., & Panagos, P. (2019). Using the USLE: Chances, challenges and limitations of soil erosion modelling. *International Soil and Water Conservation Research*, 7(3), 203–225. <https://doi.org/10.1016/j.iswcr.2019.05.004>
- Amanambu, A. C., Li, L., Egbinola, C. N., Obarein, O. A., Mupenzi, C., & Chen, D. (2019). Spatio-temporal variation in rainfall-runoff erosivity due to climate change in the lower Niger basin, West Africa. *Catena*, 172, 324–334. <https://doi.org/10.1016/j.catena.2018.09.003>
- Azari, M., Moradi, H. R., Saghafian, B., & Faramarzi, M. (2016). Climate change impacts on streamflow and sediment yield in the north of Iran. *Hydrological Sciences Journal*, 61(1), 123–133. <https://doi.org/10.1080/02626667.2014.967695>
- Baartman, J. E. M., Jetten, V. G., Ritsema, C. J., & de Vente, J. (2012). Exploring effects of rainfall intensity and duration on soil erosion at the catchment scale using openLISEM: Prado catchment, SE Spain. *Hydrological Processes*, 26(7), 1034–1049. <https://doi.org/10.1002/hyp.8196>
- Bagarello, V., Ferro, V., & Giordano, G. (2010). Testing alternative erosivity indices to predict event soil loss from bare plots in southern Italy. *Hydrological Processes*, 24(6), 789–797. <https://doi.org/10.1002/hyp.7538>
- Batista, P. V., Davies, J., Silva, M. L., & Quinton, J. N. (2019). On the evaluation of soil erosion models: Are we doing enough? *Earth-Science Reviews*, 197, 102898. <https://doi.org/10.1016/j.earscirev.2019.102898>
- Batista, P. V., Laceby, J. P., Davies, J., Carvalho, T. S., Tassinari, D., Silva, M. L., ... Quinton, J. N. (2021). A framework for testing large-scale distributed soil erosion and sediment delivery models: Dealing with uncertainty in models and the observational data. *Environmental Modelling & Software*, 137, 104961. <https://doi.org/10.1016/j.envsoft.2021.104961>
- Beasley, D. B., Huggins, L. F., & Monke, E. J. (1980). ANSWERS: A model for watershed planning. *Transactions of ASAE*, 23(4), 938–944. <https://doi.org/10.13031/2013.34692>
- Beven, K. (2006). A manifesto for the equifinality thesis. *Journal of Hydrology*, 320(1–2), 18–36. <https://doi.org/10.1016/j.jhydrol.2005.07.007>
- Beven, K. J., & Brazier, R. E. (2011). Dealing with uncertainty in erosion model predictions. In R. P. C. Morgan & M. A. Nearing (Eds.), *Handbook of erosion modelling* (pp. 52–79). Chichester, UK: Blackwell Publishing.
- Bicknell, B. R., Imhoff, J. C., Kittle, J. L., Donigian, A. S., & Johanson, R. C. (1993). *Hydrological Simulation Program - FORTRAN* (Tech. Ref.). Washington, D.C.: US Environmental Protection Agency.
- Borrelli, P., Robinson, D. A., Panagos, P., Lugato, E., Yang, J. E., Alewell, C., ... Ballabio, C. (2020). Land use and climate change impacts on global soil erosion by water (2015–2070). *Proceedings of the National Academy of Sciences*, 117(36), 21994–22001. <https://doi.org/10.1073/pnas.2001403117>
- Brazier, R. E., Beven, K. J., Freer, J., & Rowan, J. S. (2000). Equifinality and uncertainty in physically based soil erosion models: Application of the glue methodology to WEPP—the Water Erosion Prediction Project—for sites in the UK and USA. *Earth Surface Processes and Landforms*, 25(8), 825–845. [https://doi.org/10.1002/1096-9837\(200008\)25:8<825::AID-ESP101>3.0.CO;2-3](https://doi.org/10.1002/1096-9837(200008)25:8<825::AID-ESP101>3.0.CO;2-3)
- Bussi, G., Dadson, S. J., Prudhomme, C., & Whitehead, P. G. (2016). Modelling the future impacts of climate and land-use change on suspended sediment transport in the River Thames (UK). *Journal of Hydrology*, 542, 357–372. <https://doi.org/10.1016/j.jhydrol.2016.09.010>
- Centeri, C., Barta, K., Jakab, G., Szalai, Z., & Bíró, Z. (2009). Comparison of EUROSEM, WEPP, and MEDRUSH model calculations with measured runoff and soil-loss data from rainfall simulations in Hungary. *Journal of Plant Nutrition and Soil Science*, 172(6), 789–797. <https://doi.org/10.1002/jpln.200900009>
- Cerdan, O., Le Bissonnais, Y., Couturier, A., Bourennane, H., & Souchère, V. (2002). Rill erosion on cultivated hillslopes during two extreme rainfall events in Normandy, France. *Soil and Tillage Research*, 67(1), 99–108. [https://doi.org/10.1016/S0167-1987\(02\)00045-4](https://doi.org/10.1016/S0167-1987(02)00045-4)
- Chandramohan, T., Venkatesh, B., & Balchand, A. (2015). Evaluation of three soil erosion models for small watersheds. *Aquatic Procedia*, 4, 1227–1234. <https://doi.org/10.1016/j.aqpro.2015.02.156>
- Cho, S. J., Wilcock, P., & Hobbs, B. (2018). Topographic filtering simulation model for sediment source apportionment. *Geomorphology*, 309, 1–19. <https://doi.org/10.1016/j.geomorph.2018.02.014>
- Coulthard, T. J., Ramirez, J., Fowler, H. J., & Glenis, V. (2012). Using the UKCP09 probabilistic scenarios to model the amplified impact of climate change on drainage basin sediment yield. *Hydrology and Earth System Sciences*, 16(11), 4401–4416. <https://doi.org/10.5194/hess-16-4401-2012>
- Croke, J., & Nethery, M. (2006). Modelling runoff and soil erosion in logged forests: Scope and application of some existing models. *Catena*, 67 (1), 35–49. <https://doi.org/10.1016/j.catena.2006.01.006>
- de Vente, J., Poesen, J., Govers, G., & Boix-Fayos, C. (2009). The implications of data selection for regional erosion and sediment yield modelling. *Earth Surface Processes and Landforms*, 34(15), 1994–2007. <https://doi.org/10.1002/esp.1884>
- de Vente, J., Poesen, J., Verstraeten, G., Govers, G., Vanmaercke, M., Van Rompaey, A., ... Boix-Fayos, C. (2013). Predicting soil erosion and sediment yield at regional scales: Where do we stand? *Earth-Science Reviews*, 127, 16–29. <https://doi.org/10.1016/j.earscirev.2013.08.014>
- Doten, C. O., Bowling, L. C., Lanini, J. S., Maurer, E. P., & Lettenmaier, D. P. (2006). A spatially distributed model for the dynamic prediction of sediment erosion and transport in mountainous forested watersheds. *Water Resources Research*, 42(4), 1–15. <https://doi.org/10.1029/2004WR003829>
- Eekhout, J. P. C., & de Vente, J. (2019). The implications of bias correction methods and climate model ensembles on soil erosion projections under climate change. *Earth Surface Processes and Landforms*, 44(5), 1137–1147. <https://doi.org/10.1002/esp.4563>
- Eekhout, J. P. C., & de Vente, J. (2020a). How soil erosion model conceptualization affects soil loss projections under climate change. *Progress in Physical Geography: Earth and Environment*, 44(2), 212–232. <https://doi.org/10.1177/030913319871937>
- Eekhout, J. P. C., & de Vente, J. (2020b). Spatial Processes in HYdrology (SPHY) v3.0 Soil Erosion Model Ensemble. GitHub. Retrieved from [https://github.com/FutureWater/SPHY/tree/soil{\\\_\}\\_erosion{\\\_\}\\_ensemble](https://github.com/FutureWater/SPHY/tree/soil{\_\}_erosion{\_\}_ensemble)
- Eekhout, J. P. C., Hunink, J. E., Terink, W., & de Vente, J. (2018). Why increased extreme precipitation under climate change negatively affects water security. *Hydrology and Earth System Sciences*, 22(11), 5935–5946. <https://doi.org/10.5194/hess-22-5935-2018>
- Eekhout, J. P. C., Terink, W., & de Vente, J. (2018). Assessing the large-scale impacts of environmental change using a coupled hydrology and soil erosion model. *Earth Surface Dynamics*, 6(3), 687–703. <https://doi.org/10.5194/esurf-6-687-2018>

- Engelund, F., & Hansen, E. (1967). *A monograph on sediment transport in alluvial streams*. Copenhagen, Denmark: Teknisk Forlag.
- Ewen, J., Parkin, G., & O'Connell, P. E. (2000). SHETRAN: Distributed river basin flow and transport modeling system. *Journal of Hydrologic Engineering*, 5(3), 250–258. [https://doi.org/10.1061/\(ASCE\)1084-0699\(2000\)5:3\(250\)](https://doi.org/10.1061/(ASCE)1084-0699(2000)5:3(250))
- Falk, M. G., Denham, R. J., & Mengersen, K. L. (2010). Estimating uncertainty in the revised universal soil loss equation via bayesian melding. *Journal of Agricultural, Biological, and Environmental Statistics*, 15(1), 20–37. <https://doi.org/10.1007/s13253-009-0005-y>
- Faz Cano, A. (2003). El suelo de la Región de Murcia y su potencial Agrícola. In M. Esteve Selma, M. Llorens, & C. Martínez Gallur (Eds.), *Los recursos naturales de la región de murcia: Un análisis interdisciplinar* (pp. 161–170). Murcia, Spain: Universidad de Murcia, Servicio de Publicaciones.
- Garbrecht, J. D., Nearing, M. A., Zhang, J. X. C., & Steiner, J. L. (2016). Uncertainty of climate change impacts on soil erosion from cropland in central Oklahoma. *Applied Engineering in Agriculture*, 32(6), 823–836. <https://doi.org/10.13031/aea.32.11613>
- Gupta, H. V., Kling, H., Yilmaz, K. K., & Martinez, G. F. (2009). Decomposition of the mean squared error and NSE performance criteria: Implications for improving hydrological modelling. *Journal of Hydrology*, 377 (1–2), 80–91. <https://doi.org/10.1016/j.jhydrol.2009.08.003>
- Herrera, S., Fernández, J., & Gutiérrez, J. M. (2016). Update of the Spain02 gridded observational dataset for EURO-CORDEX evaluation: Assessing the effect of the interpolation methodology. *International Journal of Climatology*, 36(2), 900–908. <https://doi.org/10.1002/joc.4391>
- Jacob, D., Petersen, J., Eggert, B., Alias, A., Christensen, O. B., Bouwer, L. M., ... Yiou, P. (2014). EURO-CORDEX: New high-resolution climate change projections for European impact research. *Regional Environmental Change*, 14(2), 563–578. <https://doi.org/10.1007/s10113-013-0499-2>
- Jetten, V., Govers, G., & Hessel, R. (2003). Erosion models: Quality of spatial predictions. *Hydrological Processes*, 17(5), 887–900. <https://doi.org/10.1002/hyp.1168>
- Kimaro, D., Poesen, J., Msanya, B., & Deckers, J. (2008). Magnitude of soil erosion on the northern slope of the Uluguru Mountains, Tanzania: Interrill and rill erosion. *Catena*, 75(1), 38–44. <https://doi.org/10.1016/j.catena.2008.04.007>
- Kirkby, M., Abrahart, R., McMahon, M., Shao, J., & Thornes, J. (1998). MEDALUS soil erosion models for global change. *Geomorphology*, 24 (1), 35–49. [https://doi.org/10.1016/S0169-555X\(97\)00099-8](https://doi.org/10.1016/S0169-555X(97)00099-8)
- Krysanova, V., Vetter, T., Eisner, S., Huang, S., Pechlivanidis, I., Strauch, M., ... Hattermann, F. F. (2017). Intercomparison of regional-scale hydrological models and climate change impacts projected for 12 large river basins worldwide - a synthesis. *Environmental Research Letters*, 12, 10. <https://doi.org/10.1088/1748-9326/aa8359>
- Lazar, A. N., Butterfield, D., Futter, M. N., Rankinen, K., Thouvenot-Korppoo, M., Jarritt, N., ... Whitehead, P. G. (2010). An assessment of the fine sediment dynamics in an upland river system: INCA-Sed modifications and implications for fisheries. *Science of the Total Environment*, 408 (12), 2555–2566. <https://doi.org/10.1016/j.scitotenv.2010.02.030>
- Li, Z., & Fang, H. (2016). Impacts of climate change on water erosion: A review. *Earth-Science Reviews*, 163, 94–117. <https://doi.org/10.1016/j.earscirev.2016.10.004>
- Li, Z., Yu, J., Xu, X., Sun, W., Pang, B., & Yue, J. (2018). Multi-model ensemble hydrological simulation using a BP neural network for the upper Yalongjiang River basin, China. *Proceedings of the International Association of Hydrological Sciences*, 379, 335–341. <https://doi.org/10.5194/pahs-379-335-2018>
- Liu, G., Zhang, Q., & Yang, M. (2011). Using 7Be to trace temporal variation of Interrill and rill erosion on slopes. *Procedia Environmental Sciences*, 11, 1220–1226. <https://doi.org/10.1016/j.proenv.2011.12.183>
- Lukey, B. T., Bathurst, J. C., Hiley, R. A., & Ewen, J. (1995). SHETRAN sediment transport component: Equations and algorithms (Tech. Ref.). Newcastle, England: University of Newcastle upon Tyne.
- Maetens, W., Vanmaercke, M., Poesen, J., Jankauskas, B., Jankauskiene, G., & Ionita, I. (2012). Effects of land use on annual runoff and soil loss in Europe and the Mediterranean: A meta-analysis of plot data. *Progress in Physical Geography*, 36(5), 599–653. <https://doi.org/10.1177/0309133312451303>
- Ministerio de Fomento de España. (2015). Plan Nacional de Ortofotografía Aérea. [October 7, 2019]. Retrieved from <http://pnoa.ign.es/especificaciones-tecnicas>
- Mondal, A., Khare, D., Kundu, S., Meena, P. K., Mishra, P. K., & Shukla, R. (2015). Impact of climate change on future soil erosion in different slope, land use, and soil-type conditions in a part of the Narmada River basin, India. *Journal of Hydrologic Engineering*, 20(6), C5014003. [https://doi.org/10.1061/\(ASCE\)HE.1943-5584.0001065](https://doi.org/10.1061/(ASCE)HE.1943-5584.0001065)
- Morgan, R. P. C. (2005). *Soil erosion and conservation* (3rd ed.). Malden, MA: Blackwell Science Ltd.
- Morgan, R. P. C., & Duzant, J. H. (2008). Modified MMF (Morgan-Morgan-Finney) model for evaluating effects of crops and vegetation cover on soil erosion. *Earth Surface Processes and Landforms*, 33(1), 90–106. <https://doi.org/10.1002/esp.1530>
- Morgan, R. P. C., Quinton, J. N., Smith, R. E., Govers, G., Poesen, J. W. A., Auerswald, K., ... Folly, A. J. V. (1998b). The European Soil Erosion Model (EUROSEM): Documentation and user guide Tech. Rep. No. Version 3.6. Silsoe, United Kingdom: Silsoe College, Cranfield University.
- Morgan, R. P. C., Quinton, J. N., Smith, R. E., Govers, G., Poesen, J. W. A., Auerswald, K., ... Styczen, M. E. (1998a). The European soil erosion model (EUROSEM): A dynamic approach for predicting sediment transport from fields and small catchments. *Earth Surface Processes and Landforms*, 23(6), 527–544. [https://doi.org/10.1002/\(SICI\)1096-9837\(199806\)23:6<527::AID-ESP868>3.0.CO;2-5](https://doi.org/10.1002/(SICI)1096-9837(199806)23:6<527::AID-ESP868>3.0.CO;2-5)
- Mullan, D., Favis-Mortlock, D., & Fealy, R. (2012). Addressing key limitations associated with modelling soil erosion under the impacts of future climate change. *Agricultural and Forest Meteorology*, 156, 18–30. <https://doi.org/10.1016/j.agrformet.2011.12.004>
- Nearing, M., Deer-Ascough, L., & Laflen, J. M. (1990). Sensitivity analysis of the WEPP hillslope profile erosion model. *Transactions of ASAE*, 33 (3), 839–849. <https://doi.org/10.13031/2013.31409>
- Nearing, M. A., Foster, G. R., Lane, L. J., & Finkner, S. C. (1989). A process-based soil erosion model for USDA-Water Erosion Prediction Project technology. *Transactions of ASAE*, 32(5), 1587–1593. <https://doi.org/10.13031/2013.31195>
- Nearing, M. A., Pruski, F. F., & O'Neal, M. R. (2004). Expected climate change impacts on soil erosion rates: A review. *Journal of Soil and Water Conservation*, 59(1), 43–50. Retrieved from <http://www.jswconline.org/content/59/1/43.abstract>
- Nearing, M. A., Wei, H., Stone, J. J., Pierson, F. B., Speath, K. E., Weltz, M. A., ... Hernandez, M. (2011). A rangeland hydrology and erosion model. *Transactions of the ASABE*, 54(3), 901–908. <https://doi.org/10.13031/2013.37115>
- Nunes, J. P., Seixas, J., & Pacheco, N. R. (2008). Vulnerability of water resources, vegetation productivity and soil erosion to climate change in Mediterranean watersheds. *Hydrological Processes*, 22(16), 3115–3134. <https://doi.org/10.1002/hyp.6897>
- Nunes, J. P., Vieira, G. N., Seixas, J., Gonçalves, P., & Carvalhais, N. (2005). Evaluating the MEFIDIS model for runoff and soil erosion prediction during rainfall events. *Catena*, 61(2–3), 210–228. <https://doi.org/10.1016/j.catena.2005.03.005>
- Op de Hipt, F., Diekkrüger, B., Steup, G., Yira, Y., Hoffmann, T., & Rode, M. (2018). Modeling the impact of climate change on water resources and soil erosion in a tropical catchment in Burkina Faso, West Africa. *Catena*, 163, 63–77. <https://doi.org/10.1016/j.catena.2017.11.023>
- Pandey, A., Himanshu, S. K., Mishra, S., & Singh, V. P. (2016). Physically based soil erosion and sediment yield models revisited. *Catena*, 147, 595–620. <https://doi.org/10.1016/j.catena.2016.08.002>
- Quinton, J. N. (1997). Reducing predictive uncertainty in model simulations: A comparison of two methods using the European Soil Erosion

- Model (EUROSEM). *Catena*, 30(2–3), 101–117. [https://doi.org/10.1016/S0341-8162\(97\)00022-2](https://doi.org/10.1016/S0341-8162(97)00022-2)
- Rodríguez-Valero, M. I., & Alonso-Sarria, F. (2019). Clasificación de imágenes Landsat-8 en la Demarcación Hidrográfica del Segura. *Revista de Teledetección*, 53, 33–44. <https://doi.org/10.4995/raet.2019.11016>
- Samaniego, L., Kumar, R., Breuer, L., Chamorro, A., Flörke, M., Pechlivanidis, I. G., ... Zeng, X. (2017). Propagation of forcing and model uncertainties on to hydrological drought characteristics in a multi-model century-long experiment in large river basins. *Climatic Change*, 141(3), 435–449. <https://doi.org/10.1007/s10584-016-1778-y>
- Scholz, G., Quinton, J. N., & Strauss, P. (2008). Soil erosion from sugar beet in Central Europe in response to climate change induced seasonal precipitation variations. *Catena*, 72(1), 91–105. <https://doi.org/10.1016/j.catena.2007.04.005>
- Schürz, C., Mehdi, B., Kiesel, J., Schulz, K., & Herrnegger, M. (2020). A systematic assessment of uncertainties in large-scale soil loss estimation from different representations of USLE input factors – A case study for Kenya and Uganda. *Hydrology and Earth System Sciences*, 24(9), 4463–4489. <https://doi.org/10.5194/hess-24-4463-2020>
- Serrano-Notivoli, R., Beguería, S., Saz, M. Á., Longares, L. A., & de Luis, M. (2017). SPREAD: A high-resolution daily gridded precipitation dataset for Spain – An extreme events frequency and intensity overview. *Earth System Science Data*, 9(2), 721–738. <https://doi.org/10.5194/essd-9-721-2017>
- Shrestha, B., Babel, M. S., Maskey, S., van Griensven, A., Uhlenbrook, S., Green, A., & Akkharath, I. (2013). Impact of climate change on sediment yield in the Mekong River basin: A case study of the Nam Ou basin, Lao PDR. *Hydrology and Earth System Sciences*, 17(1), 1–20. <https://doi.org/10.5194/hess-17-1-2013>
- Shrestha, D. P., & Jetten, V. G. (2018). Modelling erosion on a daily basis, an adaptation of the MMF approach. *International Journal of Applied Earth Observation and Geoinformation*, 64, 117–131. <https://doi.org/10.1016/j.jag.2017.09.003>
- Simonneaux, V., Cheggour, A., Deschamps, C., Mouillot, F., Cerdan, O., & Le Bissonnais, Y. (2015). Land use and climate change effects on soil erosion in a semi-arid mountainous watershed (High Atlas, Morocco). *Journal of Arid Environments*, 122, 64–75. <https://doi.org/10.1016/j.jaridenv.2015.06.002>
- Stolpe, N. B. (2005). A comparison of the RUSLE, EPIC and WEPP erosion models as calibrated to climate and soil of South-Central Chile. *Acta Agriculturae Scandinavica Section B: Soil and Plant Science*, 55(1), 2–8. <https://doi.org/10.1080/09064710510008568>
- Sun, L., Fang, H., Qi, D., Li, J., & Cai, Q. (2013). A review on rill erosion process and its influencing factors. *Chinese Geographical Science*, 23(4), 389–402. <https://doi.org/10.1007/s11769-013-0612-y>
- Sun, Y., Solomon, S., Dai, A., & Portmann, R. W. (2007). How often will it rain? *Journal of Climate*, 20(19), 4801–4818. <https://doi.org/10.1175/JCLI4263.1>
- Switanek, M. B., Troch, P. A., Castro, C. L., Leuprecht, A., Chang, H. I., Mukherjee, R., & Demaria, E. M. C. (2017). Scaled distribution mapping: A bias correction method that preserves raw climate model projected changes. *Hydrology and Earth System Sciences*, 21(6), 2649–2666. <https://doi.org/10.5194/hess-21-2649-2017>
- Tebaldi, C., & Knutti, R. (2007). The use of the multi-model ensemble in probabilistic climate projections. *Philosophical Transactions of the Royal Society A: Mathematical, Physical and Engineering Sciences*, 365(1857), 2053–2075. <https://doi.org/10.1098/rsta.2007.2076>
- Teklesadik, A. D., Alemayehu, T., van Griensven, A., Kumar, R., Liersch, S., Eisner, S., ... Wang, X. (2017). Inter-model comparison of hydrological impacts of climate change on the upper Blue Nile basin using ensemble of hydrological models and global climate models. *Climatic Change*, 141(3), 517–532. <https://doi.org/10.1007/s10584-017-1913-4>
- Terink, W., Lutz, A. F., Simons, G. W. H., Immerzeel, W. W., & Droogers, P. (2015). SPHY v2.0: Spatial processes in hydrology. *Geoscientific Model Development*, 8(7), 2009–2034. <https://doi.org/10.5194/gmd-8-2009-2015>
- Thober, S., Kumar, R., Wanders, N., Marx, A., Pan, M., Rakovec, O., ... Zink, M. (2018). Multi-model ensemble projections of European river floods and high flows at 1.5, 2, and 3 degrees global warming. *Environmental Research Letters*, 13(1), 014003. <https://doi.org/10.1088/1748-9326/aa9e35>
- Tiwari, A. K., Risse, L. M., & Nearing, M. A. (2000). Evaluation of WEPP and its comparison with USLE and RUSLE. *Transactions of ASAE*, 43(5), 1129–1135. <https://doi.org/10.13031/2013.3005>
- Van Rompaey, A. J., & Govers, G. (2002). Data quality and model complexity for regional scale soil erosion prediction. *International Journal of Geographical Information Science*, 16(7), 663–680. <https://doi.org/10.1080/13658810210148561>
- van Rompaey, A. J. J., Govers, G., & Baudet, M. (1999). A strategy for controlling error of distributed environmental models by aggregation. *International Journal of Geographical Information Science*, 13(6), 577–590. <https://doi.org/10.1080/136588199241120>
- Vautard, R., Gobiet, A., Sobolowski, S., Kjellström, E., Stegehuis, A., Watkiss, P., ... Jacob, D. (2014). The European climate under a 2°C global warming. *Environmental Research Letters*, 9(3), 034006. <https://doi.org/10.1088/1748-9326/9/3/034006>
- Velázquez, J. A., Schmid, J., Ricard, S., Muerth, M. J., Gauvin St-Denis, B., Minville, M., ... Turcotte, R. (2013). An ensemble approach to assess hydrological models' contribution to uncertainties in the analysis of climate change impact on water resources. *Hydrology and Earth System Sciences*, 17(2), 565–578. <https://doi.org/10.5194/hess-17-565-2013>
- Warszawski, L., Frieler, K., Huber, V., Piontek, F., Serdeczny, O., & Schewe, J. (2014). The inter-sectoral impact model intercomparison project (ISI-MIP): Project framework. *Proceedings of the National Academy of Sciences of the United States of America*, 111(9), 3228–3232. <https://doi.org/10.1073/pnas.1312330110>
- Wicks, J., & Bathurst, J. (1996). SHESED: A physically based, distributed erosion and sediment yield component for the SHE hydrological modelling system. *Journal of Hydrology*, 175(1–4), 213–238. [https://doi.org/10.1016/S0022-1694\(96\)80012-6](https://doi.org/10.1016/S0022-1694(96)80012-6)
- Wischmeier, W. H., Johnson, C. B., & Cross, B. V. (1971). A soil erodibility nomograph for farmland and construction sites. *Journal of Soil and Water Conservation*, 26(5), 189–193.
- Woolhiser, D., Smith, R. E., & Goodrich, D. (1990). KINEROS, A Kinematic Runoff and Erosion Model: Documentation and user manual, (Tech. Ref.). Washington, D.C.: ARS, USDA.
- Xiao, H., Liu, G., Liu, P., Zheng, F., Zhang, J., & Hu, F. (2017). Developing equations to explore relationships between aggregate stability and erodibility in Ultisols of subtropical China. *Catena*, 157, 279–285. <https://doi.org/10.1016/j.catena.2017.05.032>
- Zabaleta, A., Meaurio, M., Ruiz, E., & Antigüedad, I. (2014). Simulation climate change impact on runoff and sediment yield in a small watershed in the Basque Country, northern Spain. *Journal of Environmental Quality*, 43(1), 235–245. <https://doi.org/10.2134/jeq2012.0209>
- Zhao, Y., Li, Z., Cai, S., & Wang, H. (2020). Characteristics of extreme precipitation and runoff in the Xijiang River basin at global warming of 1.5°C and 2°C. *Natural Hazards*, 101(3), 669–688. <https://doi.org/10.1007/s11069-020-03889-x>

## SUPPORTING INFORMATION

Additional supporting information may be found online in the Supporting Information section at the end of this article.

**How to cite this article:** Ekhout JPC, Millares-Valenzuela A, Martínez-Salvador A, et al. A process-based soil erosion model ensemble to assess model uncertainty in climate-change impact assessments. *Land Degrad Dev*. 2021;1–14. <https://doi.org/10.1002/lrd.3920>